

Design and Implementation of a Beam-Waveguide Mirror Control System for Vernier Pointing of the DSS-13 Antenna

L. S. Alvarez, M. Moore, W. Veruttipong, and E. Andres
Ground Antennas and Facilities Engineering Section

The design and implementation of an antenna beam-waveguide (BWG) mirror position control system at the DSS-13 34-m antenna is presented. While it has several potential applications, a positioner on the last flat-plate BWG mirror (M6) at DSS 13 is installed to demonstrate the conical scan (conscan) angle-tracking technique at the Ka-band (32-GHz) operating frequency. Radio frequency (RF) beam-scanning predicts for the M6 mirror, computed from a diffraction analysis, are presented. From these predicts, position control system requirements are then derived. The final mechanical positioner and servo system designs, as implemented at DSS 13, are illustrated with detailed design descriptions given in the appendices. Preliminary measurements of antenna Ka-band beam scan versus M6 mirror tilt made at DSS 13 in December 1993 are presented. After reduction, the initial measurements are shown to be in agreement with the RF predicts. Plans for preliminary conscan experimentation at DSS 13 are summarized.

I. Introduction

Since 1976, the NASA/JPL Deep Space Network (DSN) antennas have successfully employed the conical scan (conscan) angle-tracking technique to track spacecraft in deep space. This method nutates the entire tipping portion of the antenna, and therefore displaces the microwave beam about 0.1 dB from boresight in elevation and cross-elevation. Beam-pointing error estimates are then derived from the resultant receiver output signature. The conscan technique has persevered through the DSN upgrade from S-band (2.3-GHz) to the X-band (8.45-GHz) frequency. However, as the DSN moves toward Ka-band (32-GHz) communications, the 0.1-dB beamwidth scan radii now are reduced to about 0.0016 and 0.0009 deg for the 34- and

70-m antennas, respectively. Alternatives to the current DSN conscan method (both by mechanical and electronic means) are being investigated. They are intended to relieve the antenna axis servomechanisms of these stringent Ka-band scanning requirements and to increase the bandwidth of the beam-switching capability.

In this article, a straightforward approach is presented to Ka-band vernier pointing of the 34-m DSS-13 beam-waveguide (BWG) antenna. The scheme is to rotate one of the reflector plates in the beam-waveguide optics path in order to scan the beam. It is conceivable that an ability to scan a beam quickly may allow for a single antenna to simultaneously support multiple spacecraft at two dis-

tinct, but neighboring positions in the sky. However, at this time, the DSN's motivation for scanning a beam with a BWG mirror lies principally in potential improvements in antenna-pointing capabilities. At DSS 13, a position control system has been implemented on the last flat-plate mirror (M6) specifically for demonstrating conscan at the Ka-band frequency.

This article covers the DSS 13 beam-waveguide mirror conscan project from conceptual design through initial beam-scan measurements made in December 1993. Beam-scan versus mirror tilt angle predictions, computed from a diffraction analysis for both the Ka- and X-band frequencies, are presented. From the radio frequency (RF) predicts, mechanical and servo position control requirements are then derived. The final mechanical positioner and servo control system designs, as implemented at DSS 13, are highlighted. Specific details of the designs are given in the appendices. Antenna-pointing measurements versus mirror tilt angle were made to verify the Ka-band beam-scanning predicts. Although preliminary, the initial results are in agreement with those predicted from the RF analysis. Plans for initial conscan experimentation are summarized.

II. Beam-Scanning RF Predicts

It is well understood that tilting a mirror in a beam-waveguide (BWG) antenna, like DSS 13, results in a scanned microwave beam. Indeed, the beam shift and resulting efficiency degradation of such a misaligned system can be shown to be equivalent to that of a paraboloidal reflector with an offset feed. This latter topology was analyzed many years ago by Ruze [1].

The use of the BWG mirror to scan the beam is very straightforward and robust. The physical principles underlying the beam-scanning mechanism come from simple geometrical optics. A diffraction analysis has been done using two JPL computer programs: Physical Optics (PO) and the Geometrical Theory of Diffraction (GTD). A single mirror can be used in conjunction with any feed package at every operational frequency to scan the beam.

At DSS 13, we wanted to use this scan capability with a conscan algorithm to estimate the antenna beam-pointing errors during Ka-band tracking operations. Here we prescribed the desired beam-scan angle associated with the conscan radius, which is a function of the beamwidth of the antenna (nominally 0.1 dB). A mirror tilt angle is then found. The narrower the antenna beamwidth, the smaller will be the desired scan angle and mirror tilt angle. Even

though a scanned beam will always result in a degradation of the aperture efficiency of the antenna, it has been computed that, for X- and Ka- bands, the efficiency is reduced not more than 0.1 percent for the nominal scan angles of 0.1 dB. The curves in Fig. 1 show the relationship between the Ka-band scan angle of the electromagnetic beam of the antenna and the tilt angle of the conscan mirror at the two candidate positions (M1, M6). As shown, the Ka-band 0.1-dB beamwidth conscan radius of 0.0016 deg is achieved by tilting the M1 and M6 mirrors by 0.0375 and 0.076 deg, respectively. The reduced sensitivity of scanning the beam with either BWG reflector plate is a major advantage over direct scanning with the main antenna reflector. That is, a drastically smaller and lighter reflector surface can accomplish the desired beam scanning with a less precise positioning mechanism.

In Fig. 2, the X-band beam scan predicts are presented only for the M6 mirror. The 0.1-dB beamwidth conscan radius for X-band is 0.006 deg and the necessary mirror tilt to scan the beam is 0.365 deg. Because of its simplicity, this beam-scanning design may find application to still lower frequencies. The relevant parameters of the mechanical motion will be the limit for determining the highest and lowest frequencies for which the mirror system will be used. That is, the total stroke length of the actuator (i.e., the maximum rotation of the axes) will determine the system's lowest usable RF frequency, while the actuator position accuracy will determine its highest usable RF frequency.

III. Mirror Position Control System

A. Mirror Selection

We chose M6, the last flat-plate mirror, for demonstration at DSS 13. While M6 compares favorably to M1 by having a larger magnification factor in its mirror-rotation-to-beam-scan relationship, the main motivation for choosing M6 is the accommodating nature of its electromechanical servo positioner implementation. That is, the M6 mirror is easily accessible in the antenna pedestal room and installing a positioner at its location has minimal impact on the day-to-day station operations. The main advantage of a rotating mirror at the M1 position is that this single mirror could scan the beam of any feed in the pedestal room, much in the same manner as scanning the entire tipping structure. However, modification of the M1 mirror support structure involves taking the antenna down for a number of weeks. Due to the high subscription rate of DSS 13, the M1 mirror implementation is currently deemed unacceptable.

B. Mechanical System Requirements

A limited two-axis positioner is required for the M6 mirror above the third research and development feed position in the DSS-13 antenna pedestal room. We wished to scan the beam both at the Ka- and X-band frequencies for experimentation. The predicted X-band scan radius for the mirror is 0.365 deg; thus, the mirror positioner must have at least ± 0.365 deg of angular travel in each axis of motion for operation at X-band. Although the Ka-band scan radius is roughly one-fourth that for X-band, additional mirror travel greater than the nominal 0.365 deg is desirable for studying the feasibility of implementing a true Ka-band vernier pointing system. That is, the mirror will be used for correcting pointing errors as well as estimating them, effectively closing the RF pointing loop about the mirror. We chose a pointing-correction margin of 0.008 deg. This is five times the Ka-band conscan radius (approximately 0.0016 deg for the 34-m antenna). The predicted M6 mirror tilt angle needed to scan the beam 0.0016 deg is 0.076 deg. The total Ka-band beam scan required for experimentation is then 0.0096 deg (the conscan radius plus the pointing-correction margin); this equates to a (predicted) angular travel of 0.46 deg needed for the M6 mirror.

Lastly, when not in use as a beam scanner, the mirror must function as a standard M6 mirror in the beam-waveguide optics path. This requires that it be located and stowed at an absolutely repeatable position corresponding to the nominal optical alignment position.

C. Servo Position Control Requirements

General requirements for the M6 mirror position servo are derived from the Ka-band beam-scanning predicts. The pointing accuracy requirement is obtained from the predicted M6 tilt angle of 0.076 deg needed for conscan at Ka-band. The mirror should be able to scan the beam to at least one-tenth of this angle, or to a 0.0076-deg mirror line-of-sight position. This requirement is then broken down to a 0.005-deg upper bound for position errors in each orthogonal axis of the mirror positioner. The tracking rates required for conscan are typically slow. In the DSN, the period for the circular beam scan ranges from 32 to 128 sec. While mechanical considerations may limit scanning the main antenna reflector with periods less than 32 sec, high-speed motion of a lightweight mirror gimbal assembly should be relatively easy to achieve with appropriate actuator selection. At a minimum, the mirror positioner must be able to circular scan the beam with a period of 10 sec for experimentation.

D. Mechanical System Design Description

Initially, a simple two-axes limited-motion positioner driven by linear actuators was proposed. The proposed design incorporated a mirror that rotated about the axes behind the front surface of the mirror. The resulting offset produced an undesirable parallax error. Subsequently, the design was changed and the bearings were moved outboard of the mirror, allowing their axes to intersect with each other, the front surface of the mirror, and the RF axis. Although the revised approach results in a more complex design, the utility of the positioner for other (future) applications is enhanced by elimination of the parallax error.

The final DSS-13 configuration is illustrated in Figs. 3 and 4. The mechanical design includes three major weldments: the inner gimbal, outer gimbal, and support stand; other parts are the mirror, the stepper motor linear-driven actuators, and the stow links. With the selected actuators installed, the mechanical axes can travel ± 2 deg in the inner axis and ± 3.5 deg about the outer axis. This exceeds the operational requirements for conscan experimentation at Ka- and X-band beam scanning by a factor of four. The maximum slew rates of the mirror positioner are 6.6 and 11.5 deg per sec for the inner and outer axes, respectively. This exceeds the requirement to circular scan the beam within a period of 10 sec.

Built into the mirror structure, alongside the actuator mounts, are attachments in which stow links can be inserted. These rigid members attach via zero-clearance expandable locking pins between the rotating elements of the mechanism. Use of the zero-clearance pins allows the positioner to return to the exact position each time it is locked, so it can be used as a fixed mirror station when required. Further details of the mechanical design and hardware are given in Appendix A.

E. Servo Position Control System Design Description

Figure 5 shows a block diagram of the two-axis mirror position control system implemented at DSS 13. The inner and outer gimbal axes of rotation are denoted as the X and Y axes, respectively. The drive electronics (drive amplifiers/motor controllers, limit switches, etc.) are mounted near the mirror structure on the pedestal room ceiling, then interfaced down to a rack-mounted local control panel. Slew control of each mirror axis is available at the panel, along with a display of linear positions from linear variable differential transformers (LVDTs) mounted directly on the axis actuators. The mirror can be locally driven to the nominal alignment position (zero LVDT reading) before insertion of the stow links.

Remote position control from the DSS-13 control room is established through an RS232 interface. A rack-mounted 486 PC in the remote control room serves as the mirror position command generator/controller and angle display. Mirror position control can be accomplished either with feedback (from the LVDTs) or in an open-loop fashion (by counting motor steps). As discussed in Appendix B, both modes of operation offer more mirror position control accuracy than needed to meet the requirement of 0.005 deg. Further details of the servo position control system design and hardware are given in Appendix B.

IV. Initial Beam-Scanning Measurements

Pointing measurements were made at DSS 13 in December 1993 to validate the Ka-band beam-scanning predicts. Both planetary and broadband radio noise sources were tracked with the Ka-band array feed system installed at the F3 focus below the M6 mirror positioner. With the mirror tilted to a prescribed angle, the antenna was boresighted [2] using total (noise) power measurements made on the center horn channel of the array feed. As described in Appendix C, estimates of beam scan are computed from the measured cross-elevation and elevation pointing errors. The results are presented in Fig. 6.

The predicted slope of the beam scan magnitude versus mirror tilt angle shown in Fig. 6 differs from that shown in Fig. 1 due to a different geometry of the array feed system. The original slope predict is 47.5 to 1, corresponding to the standard horn Ka-band feed geometry. This is scaled by the ratio of 38.5 to 33.5 to account for the shorter phase-center-to-M6 mirror distance of the array feed center horn. The new predict is 55 to 1, which compares well with the best-fit slope of 54 to 1 computed from the measurements. This result is preliminary since about 30 percent of outlier measurement points were encountered during the experiment, although they are not shown in Fig. 6. Effort is currently being directed toward gaining an understanding of the outliers in terms of the errors in the beam-scan validation process. These include pointing measurement uncertainties associated with the low signal-to-noise ratios of the available Ka-band noise sources that are tracked, and errors dealing with the fact that the antenna orientation is not constant during the boresighting process.

V. Summary and Future Applications

The design and implementation of an antenna beam-waveguide mirror position control system at the DSS-13 antenna has been presented. The primary motivation for

implementing the positioner on the M6 flat-plate mirror of the beam-waveguide optics path is to demonstrate the conical scan angle-tracking method at the Ka-band operating frequency. Radio frequency beam-scan predicts versus mirror tilt angle for the M6 mirror were presented and discussed in the context of the conscan application. From both the X- and Ka-band predicts, mechanical and servo control requirements for the mirror positioner were derived. The final control system implemented at DSS 13 was highlighted with detailed mechanical and servo design descriptions given in the appendices. Initial beam-scan measurements made at the Ka-band frequency in December 1993 were presented. After reduction, the preliminary measurements were shown to be in agreement with the Ka-band predictions.

The next experiment involving the M6 mirror position control system will be the demonstration of conscan at Ka-band. The conical scan algorithm presented in [3] is currently being integrated into the PC mirror controller shown in Fig. 5. Angle generation for circular beam scanning will be computed in the control room and downloaded to each mirror's axis motor controller in the pedestal room. As shown in Fig. 5, the PC mirror controller will then be interfaced to the receiver subsystems in the DSS-13 control room. Planetary and broadband radio noise sources will be tracked to demonstrate conscan at Ka-band with system noise temperature measurements input from the station's total power radiometer subsystem. The initial conscan experimentation will utilize the array feed center horn and front end electronics. However, any (Ka-band or lower frequency) feed package may be installed underneath the M6 mirror positioner for conscan or beam-scan testing.

Further applications in antenna pointing for the M6 mirror are likely to focus on the ease of obtaining precision pointing of the small and stiff mirror gimbal assembly and the potentially high bandwidths achievable by small-scale axis servos. For example, it may be desirable to decouple the RF pointing error compensation from the antenna mechanical (azimuth and elevation) servo position loops. Here, beam-pointing error measurements obtained from either conscan or an electronic tracking error sensor (e.g., a monopulse tracking feed) installed beneath the M6 mirror can directly drive the mirror position controllers. Such a vernier pointing system will essentially close the RF beam tracking loop around the mirror itself. This will give a special performance advantage if the pointing error measurements can be accurately measured at a frequency greater than that of the antenna azimuth and elevation servo bandwidths (each currently set at 0.1 Hz at DSS 13).

Acknowledgments

The authors wish to thank Mike Thorburn for his many contributions to the project. In addition, many individuals assisted with this extensive first stage of the mirror beam-pointing control system design and implementation. Dan Bathker contributed to the initial vernier pointing system concept and application development. Alfonso Feria performed the structural analysis on the mirror positioner and Don Ohashi completed the drafting. Richard Thomas of PRC, Inc., fabricated, welded, assembled, and aligned the mirror positioner structure at Goldstone. Seyavosh Ghamari and Edwin Khachatourian of PRC led the servo drives cabling effort and assisted in the software implementation, respectively. Mike Britcliffe is acknowledged for helpful discussions on the M6 mirror alignment, and Caroline Racho assisted in the preliminary beam-scan measurements and analysis.

References

- [1] J. Ruze, "Lateral-Feed Displacement in a Paraboloid," *IEEE Trans. Antennas and Propagation*, vol. AP-13, pp. 660-665, September 1965.
- [2] L. S. Alvarez, "Analysis and Applications of a General Boresight Algorithm for the DSS 13 Beam-Waveguide Antenna," *The Telecommunications and Data Acquisition Progress Report 42-111*, vol. July-September 1992, Jet Propulsion Laboratory, Pasadena, California, pp. 48-61, November 15, 1992.
- [3] L. S. Alvarez, "Analysis of Open-Loop Conical Scan Pointing Error and Variance Estimators," *The Telecommunications and Data Acquisition Progress Report 42-115*, vol. July-September 1993, Jet Propulsion Laboratory, Pasadena, California, pp. 81-90, November 15, 1993.

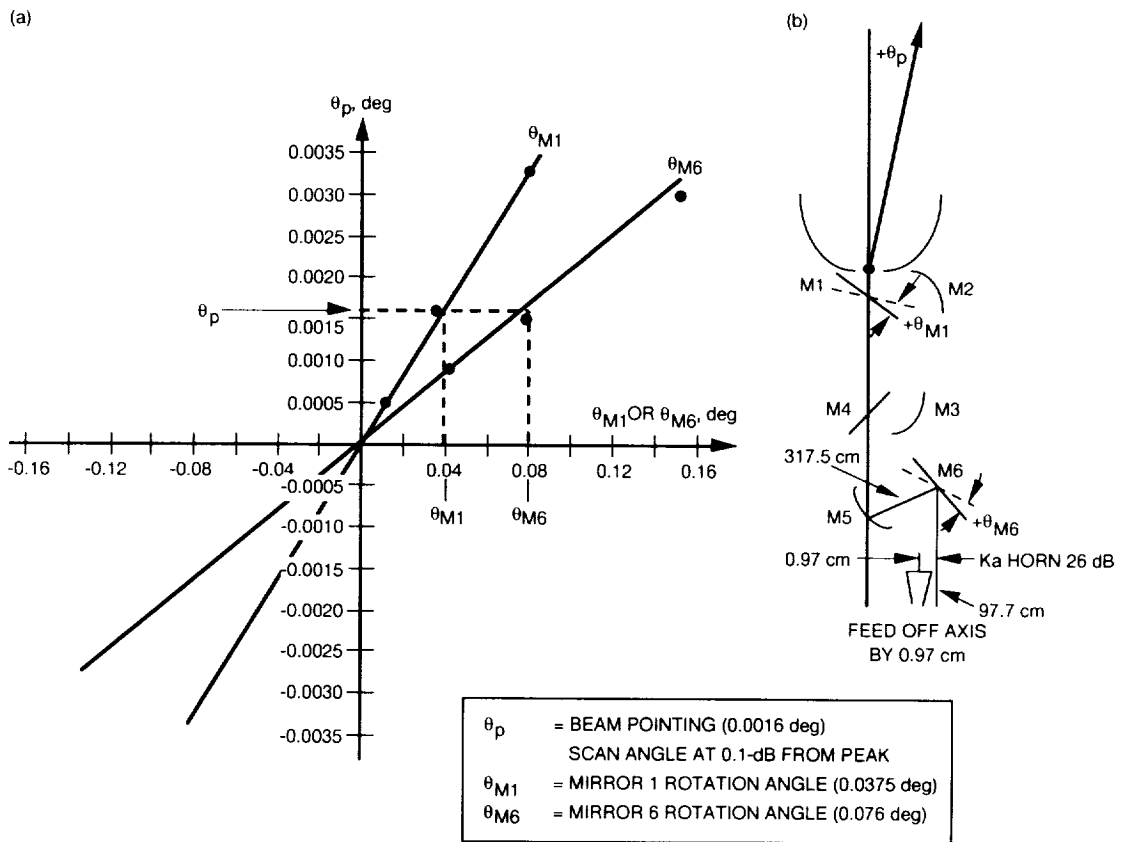


Fig. 1. RF predicts and corresponding feed geometry: (a) predicted Ka-band beam scan versus M1 and M6 mirror tilt and (b) geometry for a standard Ka-band feed at DSS 13.

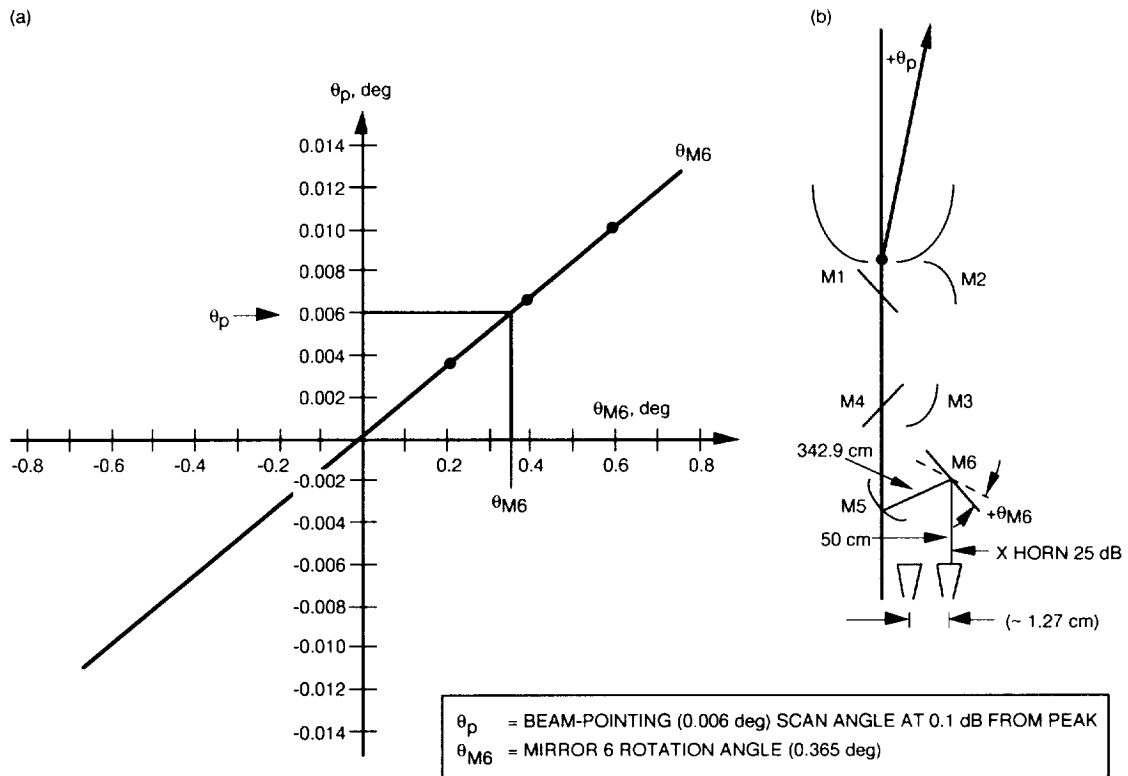


Fig. 2. RF predicts and corresponding feed geometry: (a) predicted X-band beam scan versus M6 mirror tilt and (b) geometry for a standard X-band feed at DSS 13.

ORIGINAL PAGE
BLACK AND WHITE PHOTOGRAPH

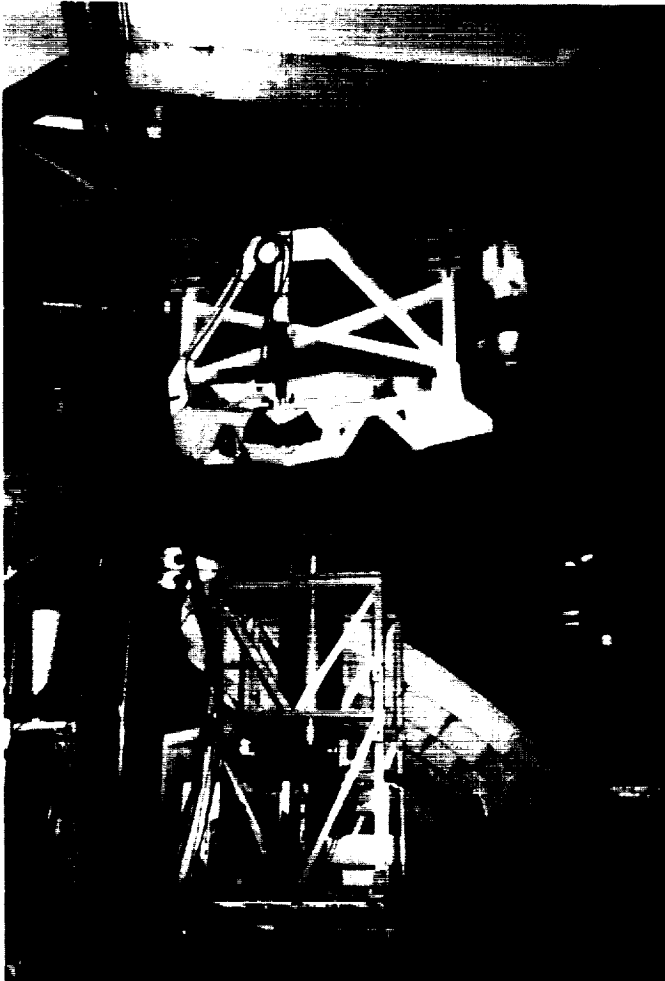


Fig. 3. The M6 mirror positioner at DSS 13, rear view.

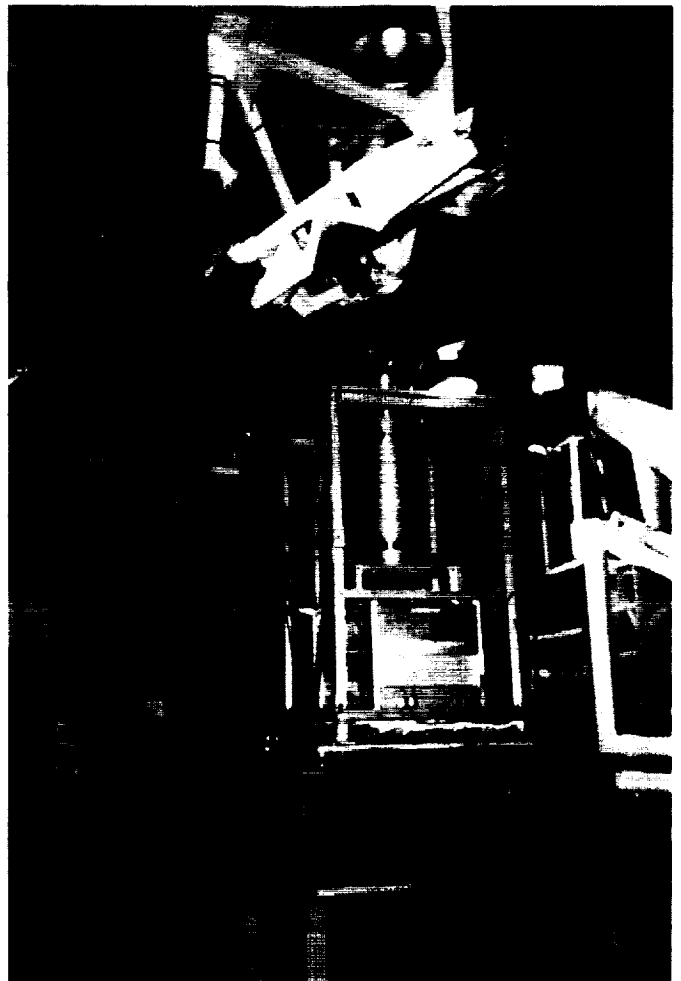


Fig. 4. The M6 mirror positioner at DSS 13, side view.

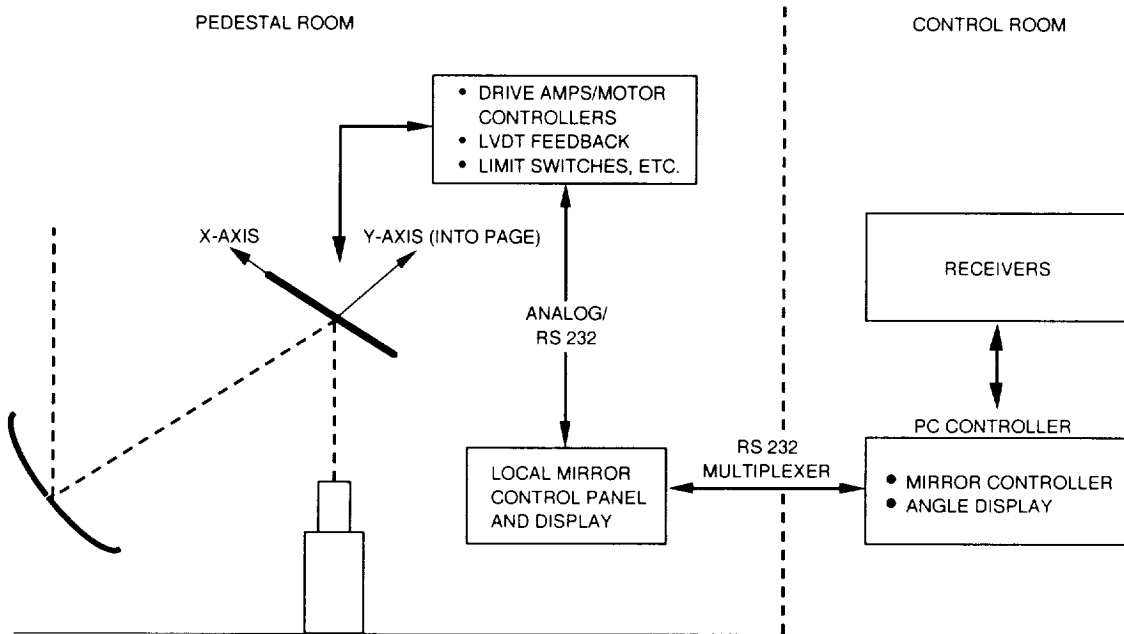


Fig. 5. Block diagram of the M6 mirror position control system at DSS 13.

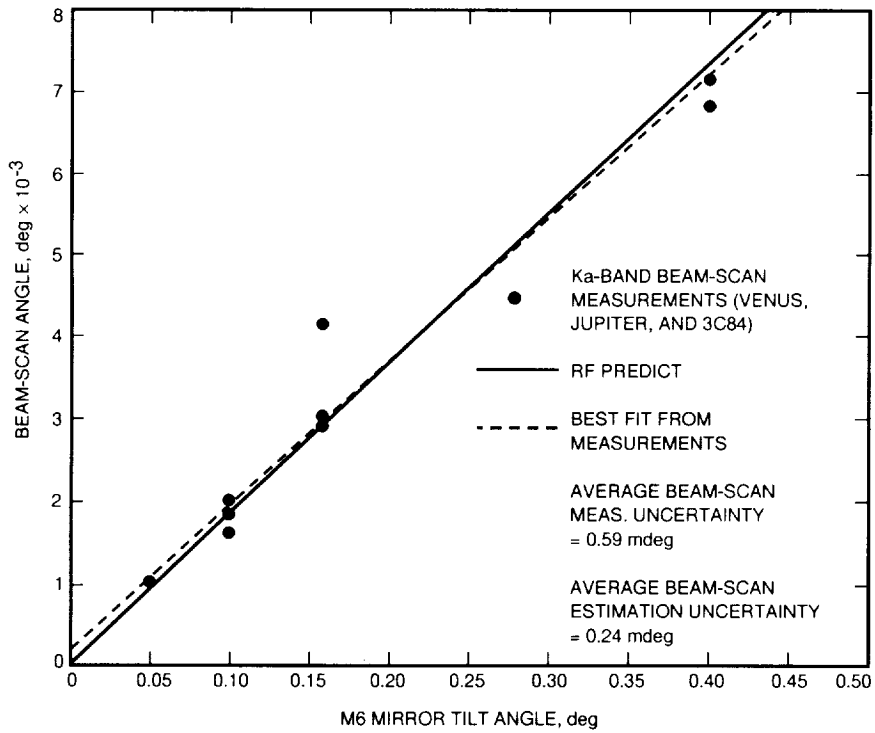


Fig. 6. Predicted and measured Ka-band beam scan versus M6 mirror tilt.

Appendix A

Mechanical Design Characteristics and Hardware Description

The overall mechanical design includes three major weldments: the inner gimbal, the outer gimbal, and support stand; other parts are the mirror, stow links, and drive actuators. These are described below.

I. Inner Gimbal

The inner gimbal is diamond shaped to provide a direct load path between the mirror and the ceiling. It is fabricated of 5- by 5- by 0.476-cm (2- by 2- by 3/16-in.) steel tubing. The inner gimbal supports the flat mirror in the center and rests within the perimeter of the outer gimbal. It attaches to the outer gimbal with bearings that are located at the top and bottom of the diamond-shaped weldments and provide the vertical axis of rotation. The bearings are shimmed for alignment with the positioner. There are also shimming provisions to adjust the mirror as required.

II. Outer Gimbal

The outer gimbal is also diamond shaped. It is fabricated of 7.6- by 7.6- by 0.635-cm (3- by 3- by 1/4-in.) steel tubing. The vertical axis bearings attach the inner gimbal to the outer gimbal at top and bottom. The horizontal axis bearings are attached at the other two corners of the outer gimbal weldment. They connect the outer gimbal to the support stand. There are shimming provisions at each of the four bearing sets that allow coplanar adjustment of the four bearings and four support yokes.

III. Support Stand

The support stand attaches to the ceiling via 7.6-cm (3-ft) plates. It also attaches to the horizontal axis bearings to the outer gimbal. There are shimming provisions to level the horizontal axis bearings.

IV. The M6 Mirror

A Blanchard ground aluminum casting was chosen over lighter more expensive alternatives. Neither weight nor inertia were considered since the positioner was designed with growth in mind and because it can position considerably greater weight than the mirror used. A dead load

midspan deflection specification of 0.005 cm (0.002 in.) was established as a criterion in the modeling. A minimum 5-cm (2-in.) thickness of the aluminum plate was indicated to satisfy this requirement.

V. Stow Links

The stow links are rigid members that attach via zero-clearance locking pins between rotating elements of the mechanism. The stow links serve two purposes:

- (1) They locate the mirror in a repeatable position, thus making it practical to use the equipment as a fixed mirror.
- (2) In the event of a control system malfunction, the actuator loads can be transferred through the links without damage to the drives or the structure. The links are located immediately next to the actuators in order to minimize the load path.

Four locking pins are used, one at each end of each stow link. They are inserted into reamed holes and have zero clearance when installed and expanded.

VI. Drive Actuators

The actuator motors step 25,000 increments per revolution. Through the gear ratio and the ball nut, this results in 793,750 steps per centimeter (312,500 steps per inch) of linear motion. Since the actuators do not back drive, they require no brakes. A small slot is provided in the motor shaft to allow it to rotate.

The key feature of the actuators, designed and built by Industrial Drives Corporation, is that they have no more than 12.7- μm (0.0005-in.) backlash at the output. The actuators use tight gear meshes and two ball nuts loaded against each other to achieve this minimal backlash.

VII. Drive Characteristics

The main drive characteristics of the mirror positioner are summarized in Table A-1. A structural analysis of the positioner was also completed. It predicts that the first structural resonance is at 8.8 Hz.

Table A-1. Drive characteristics of the DSS-13 M6 mirror positioner.

Parameter	Inner gimbal	Outer gimbal
Torque	1179.5 J (870 ft-lbs)	677.9 J (500 ft-lbs)
Moment arm	50.5 cm (19.899 in.)	88.57 cm (34.879 in.)
Maximum velocity	6.6 deg/sec	11.5 deg/sec
Acceleration	1000 deg/sec/sec	7000 deg/sec/sec
Mechanical travel	± 2 deg	± 3.5 deg/sec

Appendix B

Servo Position Control Design Characteristics and Hardware Description

I. Drive Electronics

Actuation and low-level control of the linear drive motors is accomplished using the S5201 drive indexer motor controllers from Industrial Drives Corporation. Linear position commands issued in terms of motor steps are input through an RS232 interface. The microprocessor-based controllers also provide an interface for limit switches mounted on the actuators and for remote motor jogging actuated by push-button switches on the pedestal room floor control panel. Local and remote position feedback of each actuator is accomplished by Lucas-Schaevitz 500HR linear variable differential transformers (LVDTs). One of these standard product transformers is mounted directly to the body of each actuator. The total linear range of the sensor is ± 1.27 cm (± 0.5 in.) This is discussed in terms of angular travel below. In order to return the positioner to its nominal alignment location for use as a standard fixed M6 mirror, each transformer is nulled to zero when the stow links are installed and the mirror is in the fixed station position.

II. Direct Mirror Motion Control Drive Ratios

Linear control of the stepper motors is converted into angles through moment arms of 50.5 and 88.57 cm (19.899 and 34.879 in.) for the X and Y axes, respectively. As described earlier, each actuator provides 793,750 steps per centimeter (312,500 steps per inch) of travel. Using the small angle approximation $\tan(\theta) \approx \theta$, the number of steps-to-angle ratio needed for command generation is 108,532 and 190,235 steps per degree of motion of the X and Y axes, respectively. The position errors resulting from this angle approximation are negligible for the mirror tilt angles needed to conscan at the Ka- and X-band frequencies.

III. Position Feedback and Angle Accuracy

Position feedback can be obtained either by counting commanded steps to the stepper motors or from the

LVDTs. The LVDTs are interfaced down from the ceiling into a two-channel Lucas-Schaevitz MP2000 amplifier/readout indicator. The readout indicator provides a linear motion display in the pedestal room. Each LVDT is zeroed at the nominal optical alignment position of the mirror, thus allowing local control of the mirror back to its stow position before manual insertion of the stow struts. Analog output corresponding to linear displacement for each axis is provided by the MP2000 in case a higher update rate of the position loops is desired. The DSS-13 mirror servo implementation obtains digital readouts from the MP2000 in the control room through an RS232 interface. The digital inputs for each axis are then converted to angles for terminal display and for comparison with the open-loop angle estimates computed from counting commanded motor steps.

Both the X- and Y- axis LVDTs are operated in a linear range of ± 1.27 cm (± 0.5 in.), corresponding to roughly ± 1.4 and ± 0.8 deg of travel for the X and Y axes. In this range, the chosen sensors are rated to be accurate to 2.54 to 0.254 μm (0.0001 to 0.00001 in.), which results in 0.0003 to 0.00003 deg of angular resolution for the (shorter moment arm) X axis. The number of motor steps needed to obtain the same range in resolution is from 32 down to 3. For extremely accurate position control applications, LVDT feedback is preferred since position errors caused by the motors skipping steps may become significant over time. A more significant error (when counting steps) may come from backlash at the actuator output. The maximum backlash for the actuators was stated to be 12.7 μm (0.0005 in.), or an equivalent angle error of 0.0014 deg for the X-axis. The position accuracy requirement for the beam-waveguide conscan mirror is only 0.005 deg for each axis of rotation. Thus, even under the worst-case position error scenario, pointing errors resulting from open-loop control of the stepper motors are still below the requirement.

Appendix C

Measurement Equations for the M6 Mirror

I. DSS-13 Pointing Derotation Algorithm

The geometry of the DSS-13 beam-waveguide antenna is shown in Fig. 1. During normal tracking operations, the mirror is held fixed in the pedestal room while the antenna moves independently relative to the mirror. Therefore, while tracking, fixed rotations of the mirror will not result in fixed beam-scan offsets relative to the antenna aperture. A derotation algorithm has been developed by Cramer¹ and validated at DSS 13 utilizing the array feed system. The algorithm predicts the relationship between a beam offset in the antenna aperture coordinate system and its associated phase center location in the feed position in the antenna pedestal room as a function of the antenna main reflector surface azimuth and elevation angles. The general derotation algorithm is

$$\Delta xel = -RB \cos(\phi) \quad (C-1)$$

$$\Delta el = RB \sin(\phi) \quad (C-2)$$

$$\phi = AZ - EL - \tau + \omega \quad (C-3)$$

where Δxel and Δel define a beam offset in the antenna aperture coordinate system, the radial distance R and angle ω define the phase center (in the pedestal room) associated with the offset beam given by Δxel and Δel , B is the beam deviation factor, AZ and EL are the antenna azimuth and elevation angles, and τ defines the angular position of the center of the focal plane in the pedestal room measured clockwise from true north.

II. Beam-Scan Measurement Equations

The Ka-band beam-scan predicts for small angles of rotation of the M6 mirror are given in Fig. 1. The predicts are validated by boresighting [2] the DSS-13 antenna on natural noise sources while the mirror is offset from the nominal optical alignment position. Let the beam-scan angle in Fig. 1 be denoted as Θ . It is related to the antenna aperture beam coordinates by the following expression:

$$\Theta^2 = \Delta xel^2 + \Delta el^2 \quad (C-4)$$

From the derotation algorithm above, this implies

$$\Theta = RB \quad (C-5)$$

During the tracking experiment, errors in cross-elevation and elevation are measured and then logged with the mirror tilt angle and the antenna position angles. Equation (C-4) is then used to estimate the magnitude of the beam scan. From Eqs. (C-1) and (C-2), estimates of the measured beam-scan angle can also be computed by

$$\Theta = -\frac{\Delta xel}{\cos(\phi)} \quad (C-6)$$

and

$$\Theta = \frac{\Delta el}{\sin(\phi)} \quad (C-7)$$

where ϕ is given by Eq. (C-3) and is dependent on antenna orientation.

¹ P. Cramer, "Tests of the Pointing Derotation Algorithm for DSS 13," JPL Interoffice Memorandum 3328-93-0037 (internal document), Jet Propulsion Laboratory, Pasadena, California, June 25, 1993.

Use of the Sampling Theorem to Speed Up Near-Field Physical Optics Scattering Calculations

P. W. Cramer and W. A. Imbriale
Ground Antennas and Facilities Engineering Section

Physical optics scattering calculations performed on the DSN 34-m beam-waveguide antennas at Ka-band (32 GHz) require approximately 12 hr of central processing unit time on a Cray Y-MP2 computer. This is excessive in terms of resource utilization and turnaround time. Typically, the calculations involve five surfaces, and the calculations are done two surfaces at a time. The sampling theorem is used to reduce the number of current values that must be calculated over the second surface by performing a physical optics integration over the first surface. The additional number of current values required on the second surface by subsequent physical optics integrations is obtained by interpolation over the original current values. Time improvements on the order of a factor of 2 to 4 were obtained for typical scattering pairs.

I. Introduction

The technique discussed here was developed to reduce the amount of time required by physical optics to compute the antenna patterns of the 34-m beam-waveguide antennas at the DSN. Figure 1 illustrates a typical DSN beam-waveguide (BWG) antenna. As can be seen, the antenna has eight scattering surfaces. Beginning with the feed system in the pedestal room, there is a flat mirror, an ellipse, a second flat mirror, two parabolas, a third flat mirror, the subreflector and the main reflector. However, the flat mirrors are assumed not to affect the antenna pattern properties and are ignored in the analysis, leaving five scattering surfaces. With this number of mirrors, the analysis must be repeated four times before the final far fields are evaluated. For analysis up to X-band (8.45 GHz), the available computers could easily handle calculations of such size and complexity. However, with the shift to Ka-band (32 GHz) to support future deep-space missions,

computational times are increased by a factor of about 16. Computational times of 12 hr on a Cray Y-MP2 single processor computer are typical.

This article presents a method to reduce the overall time by a factor of 4 or more for a typical pair of scattering surfaces and by a factor of 2 for the overall antenna system. The sampling theorem coupled with a near-field radial interpolation algorithm is used to speed up the physical optics calculations.

The sampling theorem has been used previously for the far-field analysis of reflecting surfaces [1]. A sampling-like technique [2] that allows the use of the Fast Fourier Transform (FFT) algorithm has been used to calculate the far fields of a parabolic reflector and the Fresnel zone fields of a planar aperture. Both methods [1] and [2] were extended to the near field [3,4], but were limited to calculating the fields on a spherical surface of constant radius.